Proceedings of the 11th International Conference on Fluid Flow, Heat and Mass Transfer (FFHMT 2024)
Chestnut Conference Centre - University of Toronto, Toronto, Canada – June 16-18, 2024
Paper No. 036
DOI: 10.11159/ffhmt24.036

Numerical Modeling Of Water-Air Multiphase Flow Within A Pipeline In The Presence Of Double Leaks

Hicham Ferroudji[1,2*], Muhammad Saad Khan[2], Abinash Barooah[3], Mohammad Azizur Rahman[2], Ibrahim Hassan[4], Rashid Hassan[3], Ahmad K. Sleiti[5], Sina Rezaei Gomari[6], Matthew Hamilton[7]

[1]Laboratory of Petroleum Equipment's Reliability and Materials, Hydrocarbons and Chemistry Faculty, Boumerdes University, Algeria.
[2]Department of Petroleum Engineering, Texas A&M University at Qatar, Qatar.
[3]Department of Petroleum Engineering, Texas A&M University, College Station, United States.
[4]Department of Mechanical Engineering, Texas A&M University at Qatar, Qatar
[5]Department Mechanical Engineering, Qatar University, Qatar.
[6]School of Computing, Engineering and Digital Technologies, Teesside University, United Kingdom.
[7]Department of Computer Science, Memorial University, Canada.
Corresponding author: Hicham Ferroudji *hichamf32@gmail.com*

Abstract **-** As the majority of petroleum businesses produce and transport gas and oil at the same time, multiphase flows are essential to the oil and gas sector. Aging, metal deterioration, and corrosion are common reasons for pipeline leaks. The energy industry not only suffers financial losses following an event, but it also raises safety and environmental issues. Thus, it becomes essential to create an effective strategy for concurrently identifying pipeline leaks. In the current work, two simultaneous leaks—one measuring 3 mm and the other 1.8 mm—in a pipeline are investigated using a 3D numerical model created with Ansys-Fluent. The experimental data obtained from a laboratory flow loop system is used to validate the numerical results. Additionally, the pipeline's flow behavior and the vicinity of the leaks are assessed. For instance, it is seen that the gas phase's escape velocity through the leaks first drops dramatically before progressively increasing to a constant value in the water tank.

Keywords**:** Turbulent flow; Multiphase flow; Double leaks; Acoustic signal; Computational fluid dynamics

1. Introduction

Industry and academia are giving this problem a lot of attention because of the possible harm that might result from pipeline breaks under specific circumstances, especially for multiphase flow. A pipeline leak has the potential to cause the transportation system to become ineffective and, if it spreads, to collapse catastrophically.

In order to replicate small water pipeline leaks, Ben-Mansour et al. (2012) employed computational fluid dynamics to create a three-dimensional turbulent flow model. The results of their investigation demonstrated that gradient and pressure varied along the pipeline. The study found that when a leak happens, the pressure signal spectrum's frequency and amplitude drastically alter, particularly in the 220-500 Hz frequency region. Furthermore, there is a noticeable shift in the mean power spectral density (PSD) in this frequency range when a leak is present.

Meng et al. (2012) proposed techniques for the identification and extraction of wave parameters from acoustic signals collected during their examination. As part of their work, they focused on locating leaks in gas pipelines using this acoustic method. They were able to differentiate between signals resulting from leaks and those caused by external disturbances by applying the wavelet transform to perform signal de-noising on the gathered data. Additionally, they suggested modifying the leak location formula to account for variations in pressure and temperature. These enhancements led to an increase in leak location accuracy.

Liu et al. (2018) used a dynamic pressure wave (DPW)-based method in their study to find and locate leaks in pipelines carrying natural gas. The wavelet transform (WT) approach was also included by the authors in their methodology. A combination of in-lab tests and practical field applications was used to validate the efficacy of these approaches. The two

methods yielded impressively low maximum absolute location errors for field leak detection: 0.725% and 0.735%, respectively.

Liu et al. (2019) investigated with the goal of creating a comprehensive model for locating and identifying failures in liquid pipelines, regardless of size. Their approach was developed using a Static Testing Module (STM) that used pressure loss to detect micro-leaks and a Dynamic Monitoring Module (DMM) that used pressure wave propagation and attenuation to detect larger leaks. Their results show that practically all leaks could be detected using the created model. With around 1% location inaccuracies.

Ayed and Hafsi's (2021) study aimed to model leak detection in a nonhomogeneous hydraulic pipeline system both experimentally and numerically. They combined mathematical model development, transient analysis, and pressure distribution analysis. They considered three leak scenarios: one leak, two leaks occurring simultaneously, and two leaks occurring sequentially. Leak locations were identified by inspecting pressure signals at the excitation location. Notably, when successive leaks occur, the study created a new method for identifying a second breach. This formula was validated using a test case.

Computational fluid dynamics (CFD) is a tool used by scientists and engineers to accurately simulate complicated interactions, dispersion, and motion of several phases within multiphase flows as computing power has increased. A number of mathematical models, including the Volume Of Fluid (VOF) model, are employed to simulate the dynamics of each phase. This technique is frequently applied in numerous industries, including the oil and gas sector, where it is used to model multiphase flow phenomena in reservoirs, pipelines, and separation operations. The versatility and potency of this strategy are becoming more and more apparent to researchers (Li et al. 2023; Wodoaski and Smoliski 2022; Mahat et al. 2023).

In the current work, multiphase flow via pipelines with two leaks is modeled using the Computational Fluid Dynamics approach. Furthermore, this considers the flow in the pipeline as well as the flow around leaks. On the other hand, experimental testing is carried out using an experimental setup (flow loop) that is equipped with various measuring techniques, including dynamic pressure sensors, in order to verify numerical results. In addition, the acoustic signals of various cases are assessed.

2. Methodology

2.1. Numerical procedure

The multiphase flow with leaks is simulated using the Volume of Fluid (VOF) model. Based on prior studies (Sun and Sakai 2016; Zahedi et al. 2014), this model would result in precise outcomes for simulating multiphase flows (water-air).

According to this method, the flow domain is characterized by a single momentum equation, and the multiphase system is determined by correlations between the volume fractions of each phase and the momentum equation's parameters, such as density and viscosity (Ansys-Fluent 2011). The mass conservation equation is represented as follows:

$$\frac{\partial P}{\partial \mathrm{t}} + \nabla.(\rho\vec{v}) = 0 \tag{1}$$

In the above equation, $\vec{v}$ represents the velocity vector.

The mass conservation equation in its general version can be used to describe an incompressible fluid flow. Moreover, the momentum conservation can written as:

$$\frac{\partial P}{\partial \mathrm{t}}(\rho\vec{v}) + \nabla.(\rho\vec{v}\vec{v}) = -\nabla p + \nabla\cdot(\bar{\tau}) + \rho\vec{g} + \vec{F} \tag{2}$$

where $\vec{g}$ and $\vec{F}$ are the gravitational body force and external body force, respectively. The stress tensor $(\bar{\tau})$ is defined as follows:

$$\bar{\tau} = \mu\left[(\nabla\vec{v} + \nabla\vec{v}^{T}) - \frac{2}{3}\nabla\cdot\vec{v}I\right] \tag{3}$$

where I is the unit tensor, is the molecular viscosity, and the impact of volume dilation is represented by the second component on the right-hand side.

On the other side, the turbulence in the multiphase flow is modeled using the "$k-\varepsilon$" approach, where the following equations represent the kinetic energy "k" and its rate of dissipation "ε":

$$\frac{\partial}{\partial t}(\rho k)+\frac{\partial}{\partial x_i}(\rho k u_i)=\frac{\partial}{\partial x_j}\left[\left(\mu+\frac{\mu_t}{\sigma_k}\right)\frac{\partial k}{\partial x_j}\right]+G_k-\rho\varepsilon+S_k \tag{4}$$

and

$$\frac{\partial}{\partial t}(\rho \varepsilon)+\frac{\partial}{\partial x_i}(\rho \varepsilon u_i)=\frac{\partial}{\partial x_j}\left[\left(\mu+\frac{\mu_t}{\sigma_\varepsilon}\right)\frac{\partial \varepsilon}{\partial x_j}\right]+G_{1\varepsilon}G_k\frac{\varepsilon}{k}-G_{2\varepsilon}\rho\frac{\varepsilon^2}{k}+S_\varepsilon \tag{5}$$

The turbulent viscosity, μ_t, can be estimated by considering the following formula:

$$\mu_t=\rho C_\mu\frac{k^2}{\varepsilon} \tag{6}$$

G_k is a term that calculates the amount of kinetic energy that turbulence produces as a result of mean velocity gradients, as follows:

$$G_k=-\rho\overline{u_i'u_j'}\frac{\partial u_j}{\partial x_i} \tag{7}$$

$G_{1\varepsilon}$, $G_{2\varepsilon}$ and C_μ are constant. S_k and S_ε are user-define source terms. σ_k and σ_ε are the turbulent Prandtl numbers for k and ε, respectively. All of these constants have the following default values in the standard $k-\varepsilon$ model (Launder and Spalding, 1972):

$G_{1\varepsilon}=1.44$, $G_{2\varepsilon}=1.92$, $C_\mu=0.09$, $\sigma_k=1$, $\sigma_\varepsilon=1$

2.2. Mesh and simulation parameters

Air-water flow in a pipeline with a diameter of 0.0508 m (2 in) and two leaks of 1.8 mm and 3 mm is analyzed numerically (Fig. 1). Furthermore, a study is conducted on the flow within the water tank as a result of leaks in order to better understand the flow via pipelines in the presence of leakage. Conversely, the geometry used in the numerical computations was designed to match the experimental configuration.

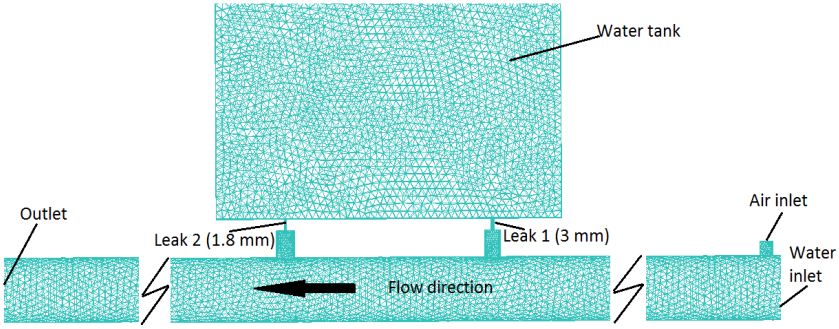

Fig. 1. Flow domain of the pipeline and water tank with two leaks.

Mesh sensitivity is carried out prior to performing numerical simulations in order to confirm that the mesh is sufficient to yield reliable results. From Fig. 2, it can be inferred that 300000 subdivisions of the flow domain are required to guarantee the accuracy of the outputs that are acquired. In order to capture the strong gradients of the computed outputs, the mesh is further improved in the vicinity of walls.

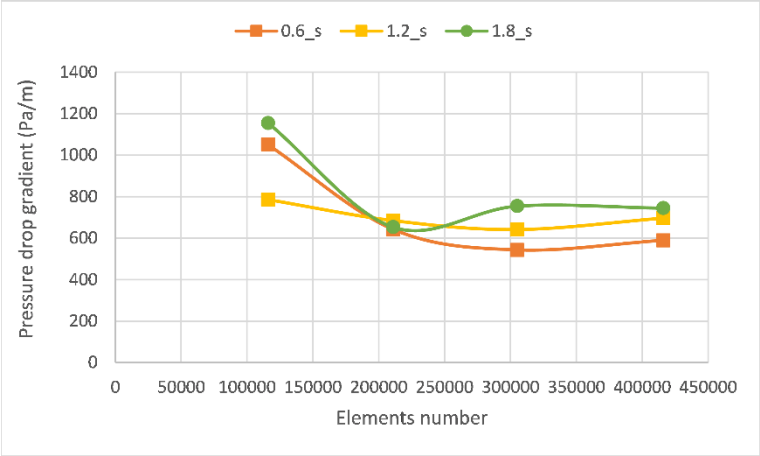

Fig. 2. Mesh sensitivity.

In terms of boundary conditions, a pressure outlet is used for the outlet and mass flow rate at the inlet is applied for both water and air (flow rates vary from 170 kg/min to 350 kg/min and from 10 g/min to 200 g/min, respectively). Additionally, the water tank is considered to be full of water.

Table 1. Parameters of numerical simulations

Parameter	Selected option
Solver	Pressure-based - Transient time scheme
Multiphase Model	Volume Of Fluid (VOF) - Sharp Interface Modeling
Phase-Interaction	Surface Tension Force Modelling (CSF) Constant Surface Tension Coefficient = 0.073 N⁄m
Turbulence Boundary Conditions	standard $k-\varepsilon$ model Inlet: imposed mass flow rate – Outlet: Outflow Walls: Non-slip conditions
Material Properties	Water: $\rho_w = 998.2\ kg/m^3$, $\mu_w = 0.001\ kg/(m \cdot s)$ Air: $\rho_A = 1.2\ kg/m^3$, $\mu_A = 1.7894e-05\ kg/(m \cdot s)$
Solution methodology	Coupling of pressure-velocity: PISO Pressure Spatial Discretization: PRESTO! Volume Fraction Spatial Discretization: Geo-reconstruct Gradients: Least-squares cell-based Other Variables: first and second-order upwind

2.3. Validation with experimental data

The numerical results are validated using experimental data from the experimental setup (Fig. 3) in the pipeline's upstream section, where the sensors are separated by 1.9 meters. Fig. 4 presents a comparison of the two strategies. The computed numerical results and the experimental data show an excellent match with a mean error of approximately 10%. This discrepancy can be attributed to the simplifications made in the numerical model, such as those in the leaks-controlling valves. These results validate the numerical model's ability to generate precise outputs and predict the gas-liquid flow in a leaky pipeline.

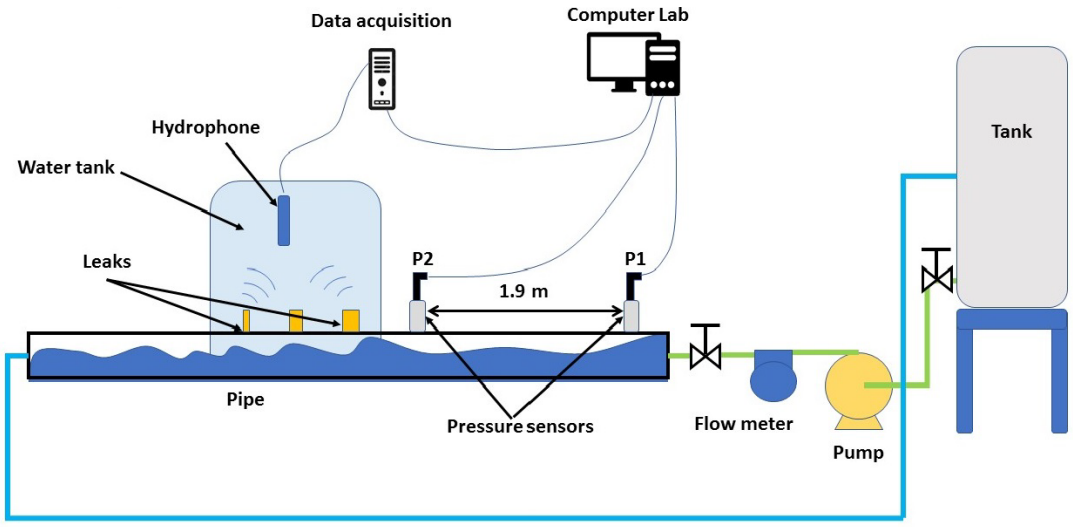

Fig.3. Experimental setup.

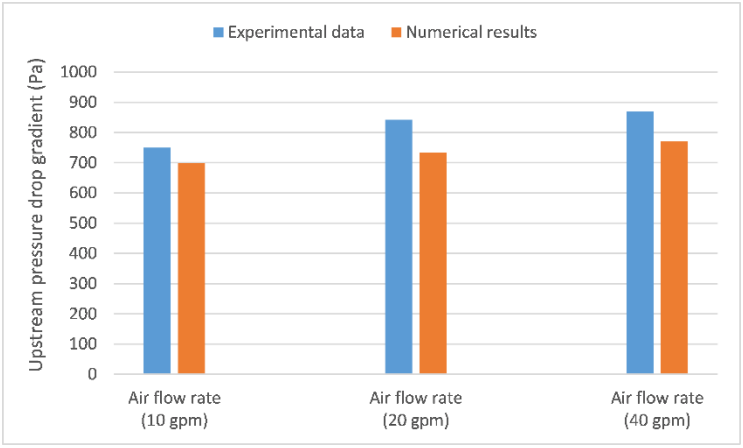

Fig.4. Validation of the numerical data (pressure drop gradient).

3. Results and discussion

The overall pressure drop gradient in the pipeline produced by leaks for gas-liquid flow at air and water flow rates of 10 to 200 g/min and 500 to 1000 g/min, respectively, is shown in Fig. 5. It is evident that as the gas flow rate increases from 10 to 200 g/min, the pressure drop gradient changes because of the properties of multiphase flow, most especially slug flow. This variation is illustrated by straight lines to show the general behavior of the pressure drop gradient inside the pipe with two leaks (1.8 mm and 3 mm). It is evident that for water running at 170 kg/min, increasing the air flow rate results in a pressure drop gradient rise of 46%, while for water flowing at 350 kg/min, this increase is estimated to be over 130%. However, at 10 g/min and 200 g/min of air flow rate, the pressure drop gradient increases by 149% and 361%, respectively, while the water flow rate increases from 170 kg/min to 350 kg/min. Because of this, the amount of air flowing through the pipeline at low water flow rates has less of an impact on the pressure drop gradient than it does at high water flow rates.

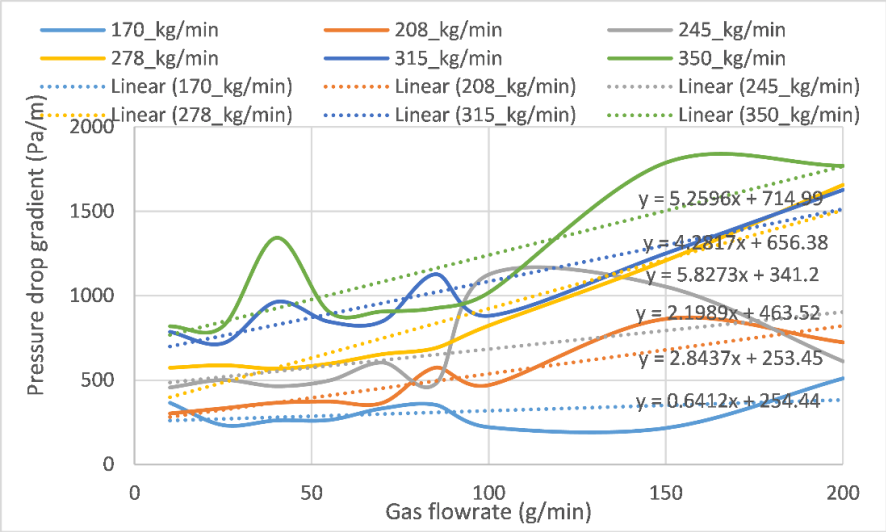

Fig. 5. Evolution of the pressure drop gradient of water-air flow through the pipeline with double leaks of 3 mm and 1.8 mm for various flow rates of water and air phases.

As seen in Fig. 6, the gas-phase flow rate in the pipeline is measured for various intake conditions of flow rates in the presence of two leaks (3 mm and 1.8 mm). The two leaks cause a dramatic change in the air-phase flow rate inside the pipeline, where it starts to decrease before reaching the first leak, as seen in this Figure. The airflow rate then reaches a constant value once the second leak is established. The occurrence of leaks in multiphase flow instances can be estimated from this behavior.

On the other hand, both instances of 170 kg/min and 245 kg/min of water flow rates have almost the same variation at the flow rate of 10 g/min of air, where the flow is reduced by 80% between the up-stream and down-stream sections of the pipeline. However, when the air flow rate at the inlet is increased to 40 g/min, the quantity of air flowability is reduced by 19% and 25% for water flow rates of 170 kg/min and 245 kg/min, respectively. This shows that the more water in the air-water multiphase system, the more air that is released through leaks. This decrease would reveal further details regarding the leaks in multiphase flow leaks.

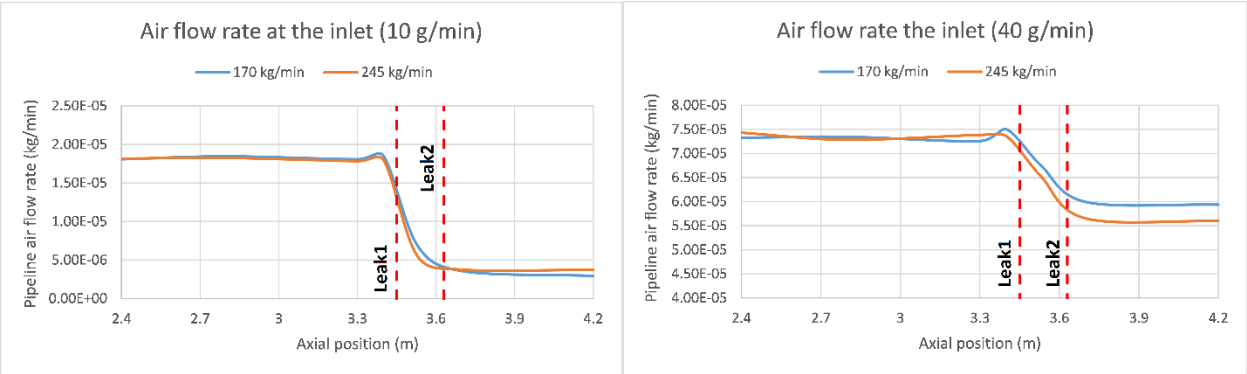

Fig. 6. Evolution of the air-phase flow rate through pipeline with double leaks of 3 mm and 1.8 mm for various flow rates of water and air phases.

The gas phase propagation in the water tank is computed for different operating conditions of the input flow rate when there are double leaks (3 mm and 1.8 mm), as Fig. 7 illustrates. In this instance, the mean velocity of the air-water system is determined using the cross-sectional area at each height of the water tank. The air velocity drops as soon as it enters the tank, as seen in Fig. 6, due to the static pressure of the water within, reaching the lowest value (0.05 m/s) at a height of 5 cm. After that, the velocity increases to reach a constant value (about 0.15 m/s) for both cases of the airflow rates of 10 g/min and 25 g/min.

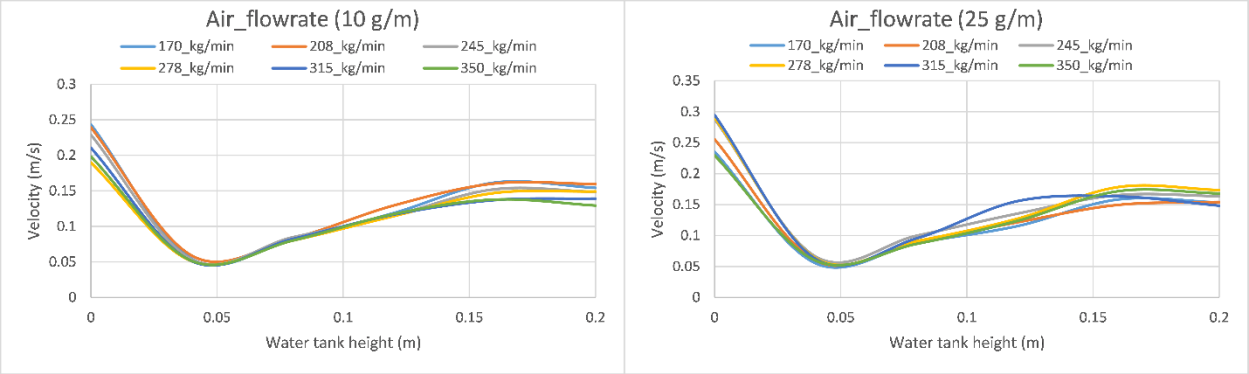

Fig. 7. Evolution of the air-phase flow rate through pipeline with double leaks of 3 mm and 1.8 mm for various flow rates of water and air phases.

Following the application of the Fast Fourier Transform (FFT) to the recorded signal at the top of the water tank, where four scenarios were taken into consideration, Fig. 8 shows the variation of the acoustic signal strength (dB) as a function of frequency. A reference acoustic pressure of 2×10^{-5} Pa has been established. As can be observed, the second case (water flow rate 350 kg/min and air flow rate 70 g/min) acoustic signal intensity exhibits larger values than the first case (water flow rate 170 kg/min and air flow rate 70 g/min), especially in the 4 kHz–5 kHz frequency range. This can be explained by the higher frequencies of the acoustic propagation from both leaks to the recording point caused by an increase in the water flow rate. The acoustic signal intensity, however, exhibits a similar trend to case 2 with lower values because of the amount of air supplied into the system when the air flow rate increases from 70 g/min to 200 g/min (case 3), while the water flow rate remains constant at 170 kg/min. As a result, the acoustic signal increases with increasing amounts of injected water.

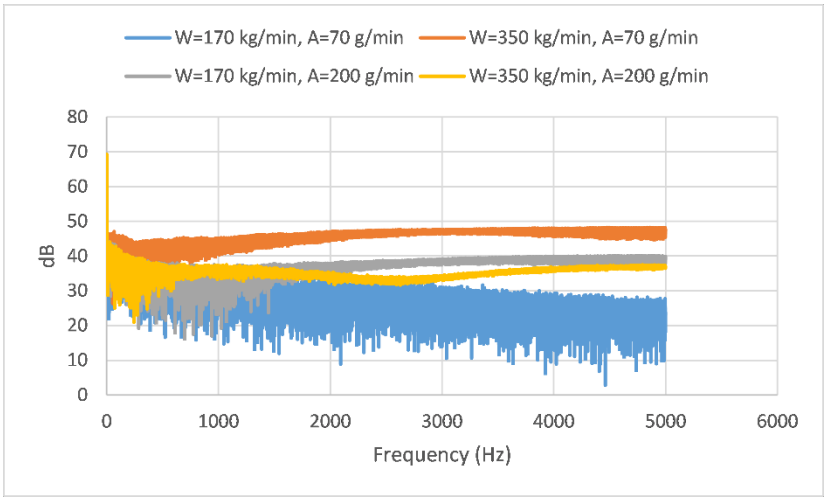

Fig. 8. Variation of the acoustic signal strength (dB) as a function of frequency.

4. Conclusion

The following briefly describes the results of the present analysis:

- Taking into account the two leaks' current operating circumstances, the water flow rate has a greater influence on the pressure drop gradient at high air flowability values.
- It is concluded that the more water in the air-water multiphase system, the more air that is released through leaks.
- The acoustic signal amplifies with increasing amounts of the injected water in the pipeline.

Acknowledgements

This publication was made possible by the grant NPRP14S-0321-210080 from the Qatar National Research Fund (a member of the Qatar Foundation). The authors will like to acknowledge QNRF for providing support and guidance without which this work would not have been possible. Statements made herein are solely the responsibility of the authors.

References

[1] Ben-Mansour, R., Habib, M. A., Khalifa, A., Youcef-Toumi, K., & Chatzigeorgiou, D. (2012). Computational fluid dynamic simulation of small leaks in water pipelines for direct leak pressure transduction. Computers & Fluids, 57, 110-123.

[2] Meng, L., Yuxing, L., Wuchang, W., & Juntao, F. (2012). Experimental study on leak detection and location for gas pipeline based on acoustic method. Journal of Loss Prevention in the Process Industries, 25(1), 90-102.

[3] Liu, C., Wang, Y., Li, Y., & Xu, M. (2018). Experimental study on new leak location methods for natural gas pipelines based on dynamic pressure waves. Journal of Natural Gas Science and Engineering, 54, 83-91.

[4] Liu, C., Li, Y., & Xu, M. (2019). An integrated detection and location model for leakages in liquid pipelines. Journal of Petroleum Science and Engineering, 175, 852-867.

[5] Ayed, L., & Hafsi, Z. (2021). Experimental and numerical investigations of multi-leaks detection in a nonhomogenous pipeline system. Arabian Journal for Science and Engineering, 46, 7729-7739.

[6] Li, S. J., Zhu, L. T., Zhang, X. B., & Luo, Z. H. (2023). Recent Advances in CFD Simulations of Multiphase Flow Processes with Phase Change. Industrial & Engineering Chemistry Research, 62(28), 10729-10786.

[7] Wodołażski, A., & Smoliński, A. (2022). Bio-hydrogen production in packed bed continuous plug flow reactor—CFD-multiphase modelling. Processes, 10(10), 1907.

[8] Mahat, M. M., Husain, H., & Mohamad, N. S. (2023). Separation efficiency analysis of multiphase flow inside hydrocyclone using CFD. Journal of Applied Engineering Design and Simulation, 3(1), 51-65.

[9] Sun, X., & Sakai, M. (2016). Numerical simulation of two-phase flows in complex geometries by using the volume-of-fluid/immersed-boundary method. Chemical Engineering Science, 139, 221-240.

[10] Zahedi, P., Saleh, R., Moreno-Atanasio, R., & Yousefi, K. (2014). Influence of fluid properties on bubble formation, detachment, rising and collapse; Investigation using volume of fluid method. Korean Journal of Chemical Engineering, 31, 1349-1361.

[11] ANSYS, I. "ANSYS Fluent Theory Guide− Release 15.0, ANSYS." (2011).

[12] Launder, B.E., Spalding, D.B., 1972. Lectures in Mathematical Models of Turbulence. Academic Press, London, England, pp. 1972.